SCIENTIFIC REPORTS

OPEN

SUBJECT AREAS:
QUANTUM PHYSICS
SUPERCONDUCTIVITY
ELECTRONIC MATERIALS AND DEVICES
NANOTECHNOLOGY

Received
07 March 2011

Accepted
03 May 2011

Published
14 June 2011

Correspondence and requests for materials should be addressed to H.B. (bouchiat@lps.u-psud.fr)

Probing the dynamics of Andreev states in a coherent Normal/Superconducting ring

F. Chiodi[1], M. Ferrier[1], K. Tikhonov[2], P. Virtanen[3], T. T. Heikkilä[3], M. Feigelman[2], S. Guéron[1] & H. Bouchiat[1]

[1]LPS, Univ. Paris-Sud, CNRS, UMR 8502, F-91405 Orsay Cedex, France, [2]L. D. Landau Institute for Theoretical Physics, Kosygin str.2, Moscow 119334, Russia, [3]Low Temperature Laboratory, Aalto University, P.O. Box 15100, FI-00076 Aalto, Finland.

The supercurrent that establishes between two superconductors connected through a normal N mesoscopic link is carried by quasiparticule states localized within the link, the "Andreev bound states (ABS)". Whereas the dc properties of this supercurrent in SNS junctions are now well understood, its dynamical properties are still an unresolved issue. In this letter we probe this dynamics by inductively coupling an NS ring to a multimode superconducting resonator, thereby implementing both a phase bias and current detection at high frequency. Whereas at very low temperatures we essentially measure the phase derivative of the supercurrent, at higher temperature we find a surprisingly strong frequency dependence in the current response of the ring: the ABS do not follow adiabatically the phase modulation. This experiment also illustrates a new tool to probe the fundamental time scales of phase coherent systems that are decoupled from macroscopic normal contacts and thermal baths.

A dissipationless current is known to flow through a thin (subnanometer) insulating barrier between two superconductors S with a superconducting phase difference, the well-known Josephson effect.[1] This supercurrent may also flow through a long (micrometer) non-superconducting metal wire at low temperatures, a spectacular consequence of the quantum phase coherence throughout the normal metal. The way the supercurrent responds to a dc phase difference, the current-phase relation,[2] was only recently measured with a Hall probe.[3] It reflects the phase dependence of the ABS,[4] entangled electron-hole states which form in the normal metal as a consequence of the superconducting mirror-like boundary conditions. Discrete phase dependent ABS were recently detected in a carbon nanotube between S electrodes[5]. In a diffusive SNS junction, with N longer than the superconducting coherence length, the ABS spectrum is a quasi-continuum of levels with a small energy gap E_g[2,7] independent of Δ. This minigap depends solely on the wire length L and the diffusion constant D, via the Thouless energy $E_{Th} = \hbar/\tau_D$, where $\tau_D = L^2/D$ is the diffusion time through the N wire. E_g is fully modulated by the phase difference φ between the superconducting order parameters on both sides: it is maximal at $\varphi = 0$ with $E_g(0) \simeq 3.1E_{Th}$ and goes linearly to zero at $\varphi = \pi$, as recently measured by scanning tunneling spectroscopy.[8] The phase dependent Josephson current $I_J(\varphi)$ at equilibrium sums the contributions of each ABS of energy ε_n, via $i_n = \frac{2e}{\hbar}\frac{\partial \varepsilon_n}{\partial \varphi}$, the current carried by level n with occupation factor p_n:

$$I_J(\varphi) = \sum_n p_n(\varepsilon_n(\varphi)) i_n(\varphi). \quad (1)$$

Its amplitude (the critical current I_c) is $11G_N E_{Th}/e$ at $T = 0$ where G_N is the normal state conductance of the normal wire and is thus independent of Δ, the superconducting gap of the electrodes. I_c decreases roughly exponentially with an increasing temperature on the scale of E_g. The phase dependence of I_J is non-sinusoidal at low temperatures, but turns sinusoidal at $T > E_g$.[2,3] This behavior presents striking analogies with persistent current of purely normal rings.[6]

Whereas the dc properties of the proximity effect (PE) at equilibrium in long SNS junctions are well understood theoretically and experimentally, its dynamics is a more complicated and yet unresolved issue. In particular the ac current response to a time dependent phase which affects both ABS energy levels and their populations still needs to be determined. At least two relaxation times should play a role, one related to the relaxation of the populations following a change of the energy levels, another related to the dynamics of the Andreev levels and possibly also a contribution due to the generation of quasiparticles. Which of the electron-electron, electron-phonon, diffusion or dephasing times are relevant in these processes? Experimentally, there are many ways in which to impose an

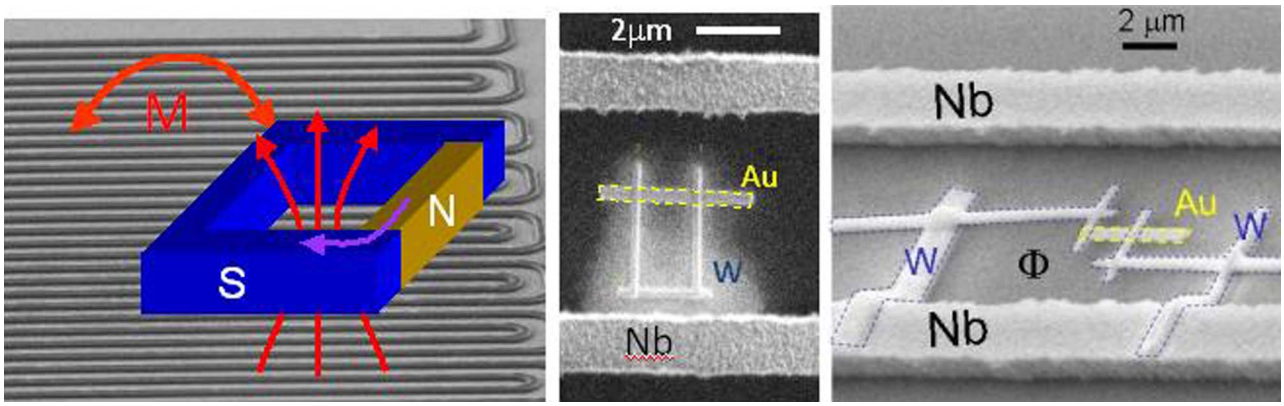

Figure 1 | Left: Principle of the experiment, the ac current in the resonator (double meander line) induces a flux modulation through the NS ring. The complex susceptibility of the ring modifies the resonator impedance. Right: Electron micrograph of the NS rings inserted in the niobium resonator, (meander line structure below). The S part large ring is attached to the resonator whereas the small one is not. This difference only affects the calculation of the inductive coupling between the ring and the resonator.

out of equilibrium situation. Because of the Josephson relation linking voltage to the time derivative of the phase, a voltage bias across the junction causes a time dependent phase and the $I(V)$ curve is a probe of the dynamics of the PE. Irradiating the junction with an RF field, which produces Shapiro steps in the $I(V)$, is another. Both the critical current in current biased experiments[9,11] and the complete dc Josephson current *vs* phase relation[3] have been shown to be very sensitive to RF excitation at frequencies of the order of or larger than $1/\tau_D$. In addition, the electron-phonon scattering rate has also been shown to set the frequency scale for the hysteresis in current biased experiments[11].

In contrast to these previous experiments on SNS junctions[3,9–11] probing the dynamics in strongly non-linear regimes, in this paper we present a linear response experiment at high frequencies. We probe the dynamics of ABS by inductively coupling an NS ring to a multimode superconducting resonator, thereby implementing both a phase bias and current detection at high frequency. Whereas at low temperature the response is essentially non dissipative and given by the flux derivative of the Josephson current a quite different behavior is observed at large temperature compared to the minigap. The frequency dependence of the response reveals, in addition to the dissipation-less current, a strong dissipative component, with a Debye-type frequency dependence and relaxation time of the order of τ_D. The dc phase dependence of the high frequency current response is very different from the dc supercurrent, and strongly non-sinusoidal. We show that this high harmonics content is well explained by phase dependent Andreev levels with a time-independent population, suggesting that the energy relaxation time is by far longer than the nanosecond time-scale probed by the experiment.

Results

The experiment consists in inductively coupling an NS ring to a multimode superconducting stripline resonator operating between 300 MHz and 6 GHz, see Figs. 1 and 2. Two different NS rings were probed, differing only by the length of the S loop.

The N part of the NS ring is a mesoscopic high purity Au wire $1.5 \times 0.3\ \mu m^2$, 50 nm thick. The estimated normal state resistance is $R_N = 1/G_N = 0.5\ \Omega$ corresponding to a conductance $g = 2 \times 10^4$ in units of $2e^2/h$. The normal wire is patterned between the resonator meander lines by e-beam lithography, and thermally evaporated onto the substrate. The S part is constructed with a W nanowire deposited using a focused ion beam. The sample is thus an ac-squid embedded in the resonator. The dc superconducting phase difference φ at the boundaries of the N wire is imposed by a magnetic flux Φ_{dc} created by a magnetic field perpendicular to the ring plane:

$$\varphi = -2\pi\mathbf{\Phi}_{dc}/\mathbf{\Phi}_0 \qquad (2)$$

with $\Phi_0 = h/2e$ the superconducting flux quantum. In addition, an ac flux $\delta\Phi_w \cos(wt)$ is generated by the ac current in the resonator. At low enough frequency the current in the NS ring should follow adiabatically the oscillating flux, and the ac response should be entirely in phase, given by the flux derivative of the Josephson current $\partial I_J(\Phi_{dc})/\partial\Phi$, also called the inverse kinetic inductance. But at high frequencies the ac current δI_w in the ring can have both an in-phase and out-of-phase response to the ac flux:

$$\delta I_w(\mathbf{\Phi}_{dc}) = \chi'(w,\mathbf{\Phi}_{dc})\delta\mathbf{\Phi}_w \cos(wt) + \chi''(w,\mathbf{\Phi}_{dc})\delta\mathbf{\Phi}_w \sin(wt), \qquad (3)$$

where $\chi = \chi' + i\chi''$, the complex susceptibility of the ring, is related to its complex admittance $Y = 1/Z$ by $\chi = iwY$. The aim of the experiment is to determine $\chi(\varphi)$ of the ring at the successive eigen-frequencies of the resonator. It is deduced from the periodic flux dependences of the resonance frequencies and inverse quality factors measured with high accuracy (see methods). It is important to distinguish the internal flux $\Phi_{\rm int}$ from the applied flux Φ_{ext} related by $\Phi_{\rm int} = \Phi_{ext} + L_g I_J(\Phi_{\rm int})$ where $L_g \sim 15$ pH is the geometrical inductance of the ring. This screening effect concerns both the ac and dc components of the flux leading to the following relation between the intrinsic susceptibility of the ring χ and the measured one χ_m:

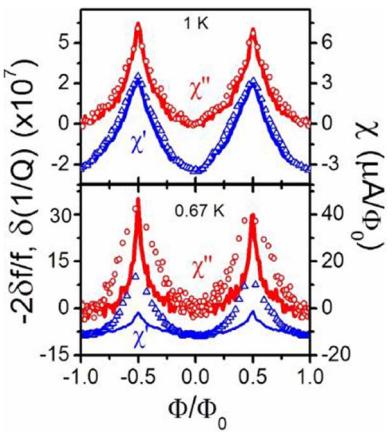

Figure 2 | Raw data $\chi'_m(\Phi_{ext})$ and $\chi''_m(\Phi_{ext})$, see Eq. (2), (thick lines) measured on the large ring, as a function of the applied external flux and same data corrected for the geometrical inductance as a function of internal flux: $\chi'(\Phi_{int})$ (triangles) and $\chi''(\Phi_{int})$ (circles), at 670 mK and 1K and $f_1 = 365$ MHz. At 1 K χ and χ_m are barely distinguishable.

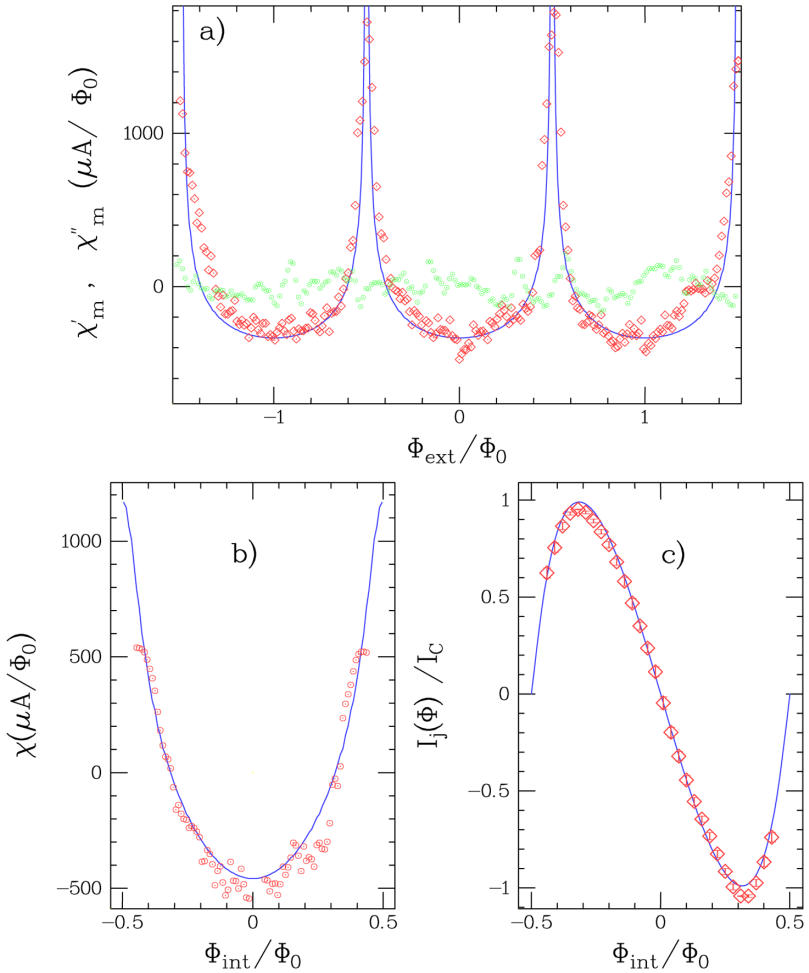

Figure 3 | (a)and (b) External and internal flux dependence of χ' measured on the small ring at 50 mK and 600 MHz in comparison with theoretical predictions assuming an adiabatic response of the ring. A quantitative agreement between theory is obtained taking $I_c = 110\ \mu$A which is comparable to the expected value $I_c = 150\ \mu\text{A} = 10.8E_{Th}/\Phi_0$. There is no detectable flux dependent signal on χ''. (c) Comparison between the integrated signal and the predicted current phase relation.

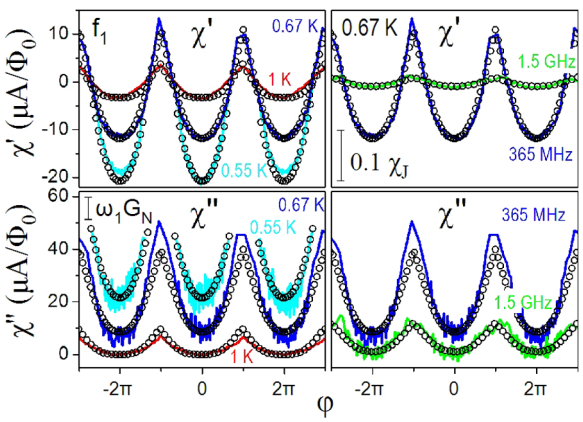

Figure 4 | Phase dependence of χ' and χ'' for different temperatures 0.55, 0.67 and 1 K all greater than the minigap and 2 different frequencies f=365MHz and 1500MHz. The amplitude of the Josephson currents calculated are $I_J(0.67\text{K}) = 18\ \mu$A and $I_J(1\ \text{K}) = 6\ \mu$A. Circles: fit with $\chi_{in}^{\infty}(\varphi,T)/(1+iw\tau)$, see expressions (5) and (6) calculated from Usadel equation[21] at temperatures corresponding to $k_BT = 5, 6$ and $8E_{Th}$ giving the best agreement with experimental data. The amplitude of the theoretical curves has been rescaled by a factor 0.3. All the curves have been arbitrarily shifted along the vertical axis.

$$\chi = \frac{\chi_m}{1 + L_g\chi_m} \tag{4}$$

These differences between $\chi_m(\Phi_{ext})$ and $\chi(\Phi_{int})$ are undetectable when L_g is small compared to the kinetic inductance (see Fig. 2 data on the large ring at 1 K). This is not the case at lower temperatures when the parameter $\beta = 2\pi L_g I_c(T)/\Phi_0$ is of the order of unity or larger. This is why we have investigated different size of rings with normal junctions of identical sizes (see Fig. 1), the small ring (L_g = 2.5 pH) is such that $\beta \leq 0.5$ down to 50 mK. The large loop ($L_g \sim 15$ pH) is more adapted to the investigation of higher temperature data since hysteresis, corresponding to $\beta \geq 1$, occurs below 600 mK. We nevertheless exploited the low temperature data on this large loop to determine the Thouless energy of the N wire which is one of the key parameters. $I_c(T)$ is first deduced from the temperature dependence of the hysteresis amplitude $\delta\Phi_{ext}(T) = 2L_gI_c(T)$. E_{Th} is then obtained from the expression of $I_c(T) \propto (k_BT/E_{Th})^{3/2}\exp\left(-\sqrt{2\pi k_BT/E_{Th}}\right)$, calculated from Ref.[14]. We find $E_{Th} = 90 \pm 10$ mK $\simeq \Delta/80$.

Below we discuss the phase dependence of $\chi(\varphi)$ with φ deduced from Φ_{int} through Eq. (2) and replacing Φ_{dc} by Φ_{int}. Fig. 3 and Fig.4 present $\chi'(\varphi)$ and $\chi''(\varphi)$ for different temperatures and resonator eigenmodes. Each curve is the average of 30 to 100 magnetic field scans. At a low temperature compared to the minigap the response is essentially non-dissipative with no oscillations detectable in $\chi''(\Phi)$. $\chi'(\Phi)$ is practically the flux derivative of the Josephson current, see

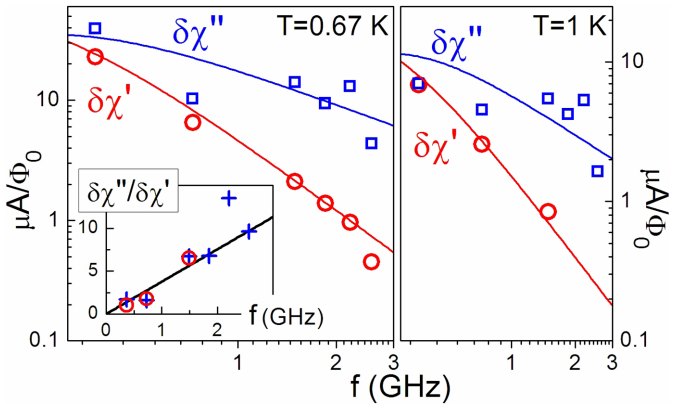

Figure 5 | Frequency dependence of $\delta\chi'$ and $\delta\chi''$ for two different temperatures above the minigap. Continuous lines: fits according to Debye relaxation laws with $\tau = 0.6$ ns. Inset: frequency dependence of the ratio $\delta\chi''/\delta\chi'$ for several temperatures. The linear dependence in $2\pi f$ confirms the validity of the Debye relaxation fits. Circles: $T = 1$ K, crosses: T=0.67 K.

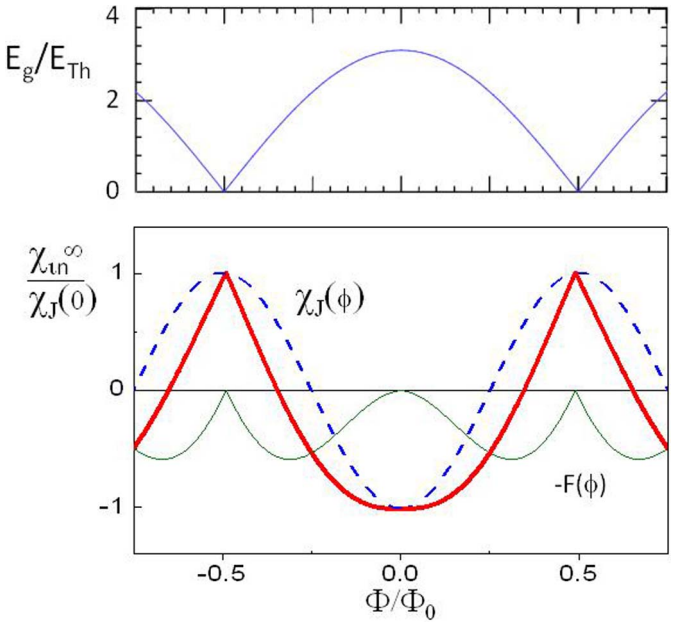

Figure 6 | Top: schematic representation of the phase dependent minigap closing linearly at $\varphi = \pi$. Bottom: dotted line, adiabatic low frequency response$\chi_0(\Phi)$ of an NS ring $\partial I_J/\partial\Phi$ at $k_BT = 8E_{Th}$. Continuous line: non-adiabatic contribution obtained when the frequency is large compared to the inverse relaxation time of the populations. $F(\varphi,T)$[19,21] was calculated using Usadel equations[20] in the limit $k_BT \gg E_{Th}$, $F(\varphi,T) \simeq \left(2\sqrt{2}\pi G_N E_{Th}/ek_BT\right)(-\pi + \mathrm{mod}(\pi+\varphi,2\pi) - \mathrm{sgn}(\sin(\varphi))\sin^2(\varphi/2/\pi)\sin(\varphi)$. Bold line: total response calculated, $\chi_{in}(\varphi) = \chi_0(\varphi) - F(\varphi,T)$, for $k_BT = 8E_{Th}$ and $w\tau_{in} = 100$, reproducing experimental results as shown on Fig. 4.

Fig. 3. A very different behavior is found at temperatures larger than $T = 0.5$ K as shown in Fig. 4. The first surprise is the observation, beside the non-dissipative response χ', of a *larger* flux dependent dissipative response χ'', over the entire frequency range investigated (365 MHz to 3 GHz). In addition, $\chi'(\varphi)$ is not a pure cosine even though the dc Josephson current is sinusoidal at these temperatures, implying that $\chi'(\varphi)$ is not simply $\chi_J(\varphi) = (2\pi/\Phi_0)\partial I_J(\varphi)/\partial\varphi$. We define the quantities $\delta\chi'$ and $\delta\chi''$ as the flux dependent parts of χ' and χ''. The frequency dependence of these quantities are plotted in Fig. 5 for different temperatures above the minigap. We find that $\delta\chi(w)$ follows a simple Debye-type dependence, $\delta\chi(w) = \delta\chi(0)/(1 + iw\tau)$, with: $\delta\chi(0)$, of the order of χ_J as expected for the $w = 0$ limit, and the relaxation time τ equal to 0.6 ± 0.2 ns, roughly 7 times τ_D. When expressed in terms of admittance like in the theoretical work in[21] $\delta Y(w) = \delta\chi(w)/iw$, our findings suggest that the flux dependent part of $\Re\delta Y(w)$ exhibits an effective Drude like frequency dependence which is independent of frequency at $w \ll 1/\tau$. We find no significant temperature dependence of τ between 0.5 and 1 K. However our low temperature results indicate that this Debye-type relaxation mechanism does not describe the dynamics below the Thouless energy.

Discussion

We now discuss possible explanations of this linear-response data at temperatures larger than the minigap. One cause of dissipation is the relaxation of the populations of Andreev levels which was invoked to explain non-equilibrium effects in voltage biased configurations such as fractional Shapiro steps.[15] This relaxation is characterized by the inelastic time τ_{in} which is the shortest of the electron-electron and electron-phonon scattering times. At temperatures larger than the minigap, it yields a frequency dependent contribution proportional to the sum over the spectrum of the square of the single level current. Note the similarity between this relaxation mechanism and the finite temperature persistent current relaxation mechanism in Aharonov Bohm mesoscopic N rings discussed in Ref.[16–18]. The susceptibility is hence

$$\chi_{in}(w) = \sum_n \left[p_n \frac{\partial i_n}{\partial\varphi} + i_n(\varphi)\frac{\partial p_n}{\partial\varepsilon_n}\frac{\partial\varepsilon_n}{\partial\varphi}\frac{1}{1+iw\tau_{in}}\right] = \frac{\partial I_J(\varphi)}{\partial\varphi} - \frac{iw\tau_{in}}{1+iw\tau_{in}}F(\varphi,T), \quad (5)$$

where the non-adiabatic contribution $F(\varphi,T) = -\sum_n \left[i_n^2 \frac{\partial p_n}{\partial\varepsilon_n}\right]$ can be written in the continuous spectrum limit in terms of the spectral current $J(\varepsilon)$ and the density $\rho(\varepsilon)$ of the the Andreev levels as: $F(\varphi,T) = \int J^2(\varphi,\varepsilon)/[k_BT\rho(\varepsilon))]d\varepsilon$. This function exhibits a sharp anomaly at $\varphi = \pi$ related to the closing of the minigap and when $w\tau_{in} \gg 1$ this anomaly contributes substantially to $\chi(\varphi)$, reproducing our experimental findings at temperatures larger than the minigap (see Figs. 4 and 6). In the temperature range of the experiment, $T \leq 1$ K, τ_{in} should be the electron-electron scattering time[24,25]. Given the S boundaries τ_{in} is probably of the order or even longer than its value in a *finite length* quasi 1D wire, itself much longer than the phase coherence time of an infinite wire or of the same wire connected to normal reservoirs. Since in the experiment $T \ll gE_{Th}/k_B \simeq 1000$K, $\tau_{in}(T) \simeq g\hbar/k_BT \simeq 100$ ns at 1 K, much longer that the nanosecond time scales investigated. Thus already at MHz frequencies Andreev level populations do not relax and are effectively frozen at their dc values. Equation 5 leads to $\chi'_{in} \approx \chi^{\infty}_{in}(\varphi,T) = \sum_n \left[p_n \frac{\partial i_n}{\partial\varphi}\right]$ and $\chi''_{in} = F(\varphi)/w\tau_{in}$ in this limit.

Whereas the above model describes the measured phase dependence $\chi'(\varphi)$ quite well (Fig. 4) for the large temperature data, it predicts a frequency independent amplitude in the investigated frequency range, which is not what is observed experimentally. Moreover the predicted χ'' is more than two orders of magnitude smaller than the experimental values and has a predominant π periodic component (due to the squared spectral current in the non-adiabatic contribution) which contrasts with the 2π measured periodicity. The experimental Debye relaxation of Fig. 5 must therefore be due to a second, different relaxation time τ much shorter than τ_{in}. It is indeed expected that as the driving frequencies become of the order of the inverse diffusion time, the Andreev levels cannot follow the phase oscillations. The relevance of the diffusion time for superconductivity in a disordered superconductor in the vicinity of T_c was already discussed long ago[9,22]. The authors found an effective

Ginzburg-Landau time in a finite wire $\tau_{GL} = (\pi^2/4)\tau_D$. This justifies to fit the experimental results at $w \gg 1/\tau_{\rm in}$ with

$$\chi(w,\varphi,T) = \chi_{\rm in}^{\infty}(\varphi,T)/(1+iw\tau). \quad (6)$$

We show in Fig. 4 that the phase dependence of χ' and χ'' are well reproduced by Eq. (6) with $\tau = 0.6$ ns and $\chi_{\rm in}^{\infty}(\varphi)$, the infinite frequency limit of (5). We use a single rescaling factor 0.3 for all data, attributed to errors in the estimation of the mutual inductance between the ring and the resonator. Recent work[26] on the finite frequency response of a SINIS junction where the N mesoscopic wire is isolated from the electrodes by an insulating barrier lead to a frequency dependent response with a characteristic time proportional to τ_D and similar flux dependences for χ' and χ'', as observed here. These results refer to the situation of temperature above the minigap, since its value is strongly suppressed by tunnel barriers. On the other hand, the computation of the high frequency impedance of a SNS junction with highly transmitting N/S interfaces recently performed in[21] emphasizes the excitation of quasiparticles above the minigap as another dissipation mechanism. These results agree with our low temperature data and high temperature data at moderate frequency but the Debye-type frequency dependence relaxation is not reproduced. Thus it seems plausible that the unexpected dissipation mechanism we found is related with diffusion of thermally excited (above the minigap) quasiparticles across the N part of the structure.

In conclusion we have measured the high frequency linear response of NS rings. At $k_BT \ll E_g$ the response is essentially non-dissipative and given by the flux derivative of the Josephson current. At $k_BT \gg E_g$ our results show the existence of a strong dissipative component in addition to the expected dissipationless current. Moreover we also observe a strong frequency variation of the flux dependent kinetic inductance beyond adiabaticity, revealing the existence of two different relaxation times: (i) The inelastic relaxation time of the populations of the Andreev levels, much longer than the experimental investigated time scales. It explains the harmonics content of the dc flux dependence of $\chi'(\Phi)$ resulting from the freezing of those populations which do not follow the time dependent flux, (ii) Another, much faster time scale, responsible for the observed dissipative response $\chi''(\Phi)$ and the high frequency decrease of $\chi'(\Phi)$ related through a Debye-type frequency dependence. This second temperature independent time scale in the ns range may be related to the diffusion time through the N segment. On the theory side, this calls for finding a relaxation time scale of the order of the diffusion time, which does not naturally show up in the frequency dependent Usadel equations in[21]. We also show that the phase dependent dynamics of a N wire between S reservoirs is fundamentally different from the dynamics of the same N wire between normal reservoirs. These measurements revealing the dynamics of the Andreev states could be extended to a wide range of SNS systems where the N part may be a semiconducting nanowire, a carbon nanotube, or a graphene ribbon.

Methods

Resonator and measurement of the susceptibility of the ring. The resonator is made of two parallel superconducting Nb meander lines (2 μm wide, $L_R = 20$ cm long, and 4 μm apart, see Fig. 1) on a sapphire substrate [12]. One line is weakly coupled to a RF generator via a small on chip capacitance, adjusted to preserve the high Q of the resonator (80 000 at 20 mK), the other one is grounded. The resonance conditions are $L_R = \frac{n\lambda_n}{2}$, where n is an integer and λ_n the electromagnetic wavelength. The fundamental resonance frequency f_1 is 365 MHz. We were able to detect more than 30 harmonics. The resonator is enclosed in a gold plated stainless-steel box, shielding it from electromagnetic noise, and cooled to mK temperature. The high Q ensures an extreme sensitivity: $\frac{\delta f}{f} \sim \delta Q^{-1} \sim 10^{-9}$, enabling very accurate ac impedance measurements of mesoscopic objects. This technique inspired by experiments performed at lower frequency on short Josephson junctions[27,28] was previously employed in contactless measurements of purely normal (N) Aharonov Bohm rings.[12] A single NS ring gives more signal than 10^4 N rings, for two reasons: First, the supercurrent in an NS ring is g times larger than the persistent current in a N ring of the same size as the N wire. Second, the length of the S wire can be adjusted to optimize the ring/resonator coupling. The dc flux dependent susceptibility is deduced from the flux induced variations in the resonance frequencies and inverse quality factors $\delta f_n(\Phi_{dc})$ and $\delta Q_n^{-1}(\Phi_{dc})$ of the resonator:

$$\frac{\delta f_n}{f_n} = -\frac{1}{2}k_n\frac{M^2}{\mathcal{L}}\chi'_m,\ \delta\frac{1}{Q_n} = k_n\frac{M^2}{\mathcal{L}}\chi''_m. \quad (7)$$

Here $\mathcal{L} = 0.15\ \mu$H is the resonator inductance, the mutual inductance between the ring and the two resonator lines was $M \sim 5$ pH and 0.2 pH for the large and the small rings, respectively, and k_n accounts for the spatial dependence of the ac field amplitude at frequency f_n.

SNS junctions using a focused ion beam. The superconducting electrodes on both sides of the Au wire are made from W nanowires deposited using a focused Ga ion beam (FIB) to decompose a tungstene carbonyle vapor. The superconducting transition temperature of these W wires is 4 K, their critical current is 1 mA, and critical field is greater than 7 T.[29] The superconducting gap measured by scanning tunneling spectroscopy[30] is $\Delta = 0.8$ meV. This technique provides a good NS interface, thanks to the light etching concomitant to the W deposition. We have checked that SNS junctions fabricated using this technique exhibit supercurrents and Shapiro steps comparable to long SNS junctions made with more conventional techniques.[13]

1. Josephson, B.D. Possible new effects in superconductive tunneling. *Phys. Lett.* **1**, 251 (1962).
2. Heikkilä, T. T. Särkkä, J. and Wilhelm, F. K. Supercurrent-carrying density of states in diffusive mesoscopic Josephson weak links. *Phys. Rev. B* **66**, 184513 (2002).
3. Fuechsle, M. *et al.* Effect of microwaves on the current-phase relation of superconductornormal-metalsuperconductor Josephson junctions. *Phys. Rev. Lett.* **102**, 127001 (2009).
4. Kulik, I. Macroscopic quantization and proximity effect in S-N-S junctions. *Sov. Phys. JETP* **30**, 944 (1970).
5. Pillet, J-D., *et al.* Andreev bound states in supercurrent-carrying carbon nanotubes revealed. *Nat. Phys.* **6**, 965 (2010).
6. Büttiker, M and Klapwijk, T. M. Flux sensitivity of a piecewise normal and superconducting metal loop. *Phys. Rev. B* **33**, 5114 (1986).
7. Zhou, F., Charlat, P., Spivak, B., and Pannetier, B. Density of states in superconductor-normal metal-superconductor junctions. *J. Low Temp. Phys.* **110**, 841 (1998).
8. le Sueur, H. *et al.* Phase controlled superconducting proximity effect probed by tunneling spectroscopy. *Phys. Rev. Lett.* **100**, 197002 (2008).
9. Warlaumont, J.M., *et al.* Microwave-enhanced proximity effect in superconductor-normal-metal-superconductor microjunctions. *Phys. Rev. Lett.* **43**, 169 (1979).
10. Lehnert, K.W., *et al.* Nonequilibrium ac Josephson effect in mesoscopic Nb-InAs-Nb junctions. *Phys. Rev. Lett.* **82**, 1265 (1999).
11. Chiodi, F., Aprili, M., and Reulet, B. Evidence for two time scales in long SNS junctions. *Phys. Rev. Lett.* **103**, 177002 (2009).
12. Deblock, R., *et al.* Ac electric and magnetic responses of nonconnected Aharonov-Bohm rings. *Phys. Rev.* **B 65**, 075301 (2002).
13. Chiodi, F., PHD thesis, Orsay 2010, and F.Chiodi, et al. unpublished.
14. Dubos, P. *et al.* Josephson critical current in a long mesoscopic S-N-S junction. *Phys. Rev. B* **63**, 064502 (2001).
15. Argaman, N. Nonequilibrium ac Josephson effect in wide mesoscopic S-N-S junctions. *Superlattices Microstruct* **25**, 861 (1999).
16. Trivedi, N. and Browne, D.A. Mesoscopic ring in a magnetic field: Reactive and dissipative response. *Phys. Rev. B* **38**, 9581 (1988).
17. Reulet, B. and Bouchiat, H. Ac conductivity of mesoscopic rings: the discrete-spectrum limit. *Phys. Rev. B* **50**, 2259 (1994).
18. Kamenev, A., Reulet, B., Bouchiat, H. and Gefen, Y. Conductance of Aharonov-Bohm rings: from the discrete spectrum to the continuum spectrum limit. *Europhys. Lett.* **28**, 391 (1994).
19. Lempitsky, S.V. Stimulation of superconductivity by a direct current in a superconductor-normal metal-superconductor junction. *Sov. Phys. JETP* **58**, 624 (1983).
20. Usadel, K.D. Generalized diffusion equation for superconducting alloys. *Phys. Rev. Lett.* **25**, 507 (1970).
21. Virtanen, P., Cuevas, J.C., Bergeret, F.S., and Heikkilä, T.T. Linear ac response of diffusive SNS junctions. *Phys. Rev. B* **83**, 144514 (2011).
22. Skocpol, W.J. and Tinkham, M. Fluctuations near superconducting phase transitions. *Rep. Prog. Phys.***38** 1049, (1975).
23. Virtanen, P., Heikkilä, T.T., Bergeret, F.S., and Cuevas, J.-C. Theory of microwave-assisted supercurrent in diffusive SNS junctions. *Phys. Rev. Lett.* **104**, 247003 (2010).
24. Blanter, Y. Electron-electron scattering rate in disordered mesoscopic systems. *Phys. Rev. B***54** 12807, (1997).
25. Texier, C. and Montambaux, G. Dephasing due to electron-electron interaction in a diffusive ring. *Phys. Rev. B* **72**, 115327 (2005).
26. Tikhonov, K. M.Sc. diploma thesis (in Russian): http://qmeso.itp.ac.ru/Publications/Manuscripts /tikhonov_diplom_2009.pdf; Tikhonov, K. and Feigel'man, M. (to be published)

27. Rifkin, R. and Deaver, B.S. Current-phase relation and phase-dependent conductance of superconducting point contacts from rf impedance measurements. *Phys. Rev. B* **13**, 3894 (1976).
28. Busch, C., Merkt, U., Grajcar, M., Plecenik, T., and Ilichev, E. Supercurrent-phase relationship of a Nb/InAs(2DES)/Nb Josephson junction in overlapping geometry. *Phys. Rev. B* **71**, 052506 (2005).
29. Kasumov, A.Yu. *et al.* Proximity effect in a superconductor-metallofullerene-superconductor molecular junction. *Phys. Rev. B* **72**, 033414 (2005).
30. Guillamon, I. *et al.* Nanoscale superconducting properties of amorphous W-based deposits grown with a focused-ion-beam. *New J. Phys.* **10** 093005, (2008).

Acknowledgements

We acknowledge A. Kasumov and F. Fortuna for help with the FIB as well as useful discussions with R. Deblock, M. Aprili, B. Reulet and L. Glazman. TTH acknowledges funding from the Academy of Finland and European Research Council (Grant No. 240362-Heattronics).

Author contributions

F.C. made the samples with the help of S.G and M.F, she conducted most of the experiments and analysed data, M.F, S.G. and H.B. designed and optimized the experimental setup, took part to the experiments and wrote most of the paper. K.T., P.V., T.H. and M.F. worked on the theory and participated in the writing of the paper.

Additional information

Supplementary Information accompanies this paper at http://www.nature.com/scientificreports

Competing financial interests: The authors declare that they have no competing financial interests.

How to cite this article: Chiodi, F. *et al.* Probing the dynamics of Andreev states in a coherent Normal/Superconducting ring. *Sci. Rep.* **1**, 3; DOI: 10.1038/srep00003 (2011).